DenseNet121-Powered Histopathological Image Analysis for Accurate Lung Cancer Detection

Sandeep Ruttala[1], Sai Shanmukh Ulli[2], Koralla Dasaanjaneya[3] and S Jayasankar[4]
{itssandeepruttala@gmail.com[1], saishanmukhulli@gmail.com[2], koralladasaanjaneya@gmail.com[3], s3.jayasankar@gmail.com[4]}

Department of CSE, VFSTR Deemed to be University, Vadlamudi, Guntur, Andhra Pradesh, India[1, 2, 3, 4]

Abstract. Lung cancer is one of the most common causes of cancer-related fatalities worldwide, and its impact on healthcare systems is growing. While histopathological analysis is still the gold standard for diagnosis, it is subjective and time-consuming due to its heavy reliance on pathologists' knowledge. Deep learning methods have been popular in medical imaging due to the need for automated, effective, and precise diagnostic tools. In this work, deep learning models for automatic histopathology image categorization are investigated, including VGG19, InceptionV3, ResNet, ViT, and DenseNet121. 15,000 photos from the Kaggle "Lung and Colon Cancer Histopathological Images" dataset, which covers several histological subtypes of lung cancer, make up the dataset employed. To increase the generalization of the model, data preprocessing includes resizing, augmentation, and standardization. The models are assessed using a variety of performance metrics, including accuracy, precision, recall, F1 score, confusion matrix, and ROC curves. They are trained using the Adam optimizer with a learning rate of 1e-4. The experimental findings show that deep learning models can detect lung cancer with high accuracy, indicating their potential to help pathologists make an accurate and timely diagnosis. This method improves patient outcomes by decreasing reliance on manual examination, which opens the door to quicker and more reliable cancer detection. To guarantee their use in clinical practice, more research can improve these models using explainable AI techniques.

Keywords: Lung Cancer, Deep Learning, Histopathological Images, VGG19, ResNet, ViT, DenseNet121, CNN, Machine Learning.

1 Introduction

Lung cancer is one of the most common and serious cancers, and about 80% of lung cancer deaths are caused by tobacco smoking. According to the World Health Organization (WHO) [1], lung cancer is predicted to lead to 1.8 million deaths annually, further emphasizing the importance of early and accurate detection for patient survival. Histopathological study of tissue is still the gold standard for lung cancer diagnoses and has been routinely used in conventional diagnostic approaches. The diagnosis is definitive with histology; however, manual read-out of these tissue images is time-consuming, subjective, and prone to inter-observer variation, with a risk for interference with the agreement and reliability of the diagnosis.

In the last years, deep learning and AI in general have become increasingly powerful for analysing medical images, particularly, histopathologic images. Thanks to these technologies the analysis of complex patterns in lung tissue scans can be performed in an automatic and accurate way. Recently, the development of CNN achieved remarkable improvement in the

ICITSM-Part I 2025, April 28-29, Tiruchengode, India

DOI 10.4108/eai.28-4-2025.2357810

features extraction and classification performance compared with standard methods. And contextual and long-range dependencies among histopathological images can also be encoded by transformer-based models such as Vision Transformers (ViTs) which might further improve the effectiveness of diagnosis. By such models-based systems, an automated lung cancer detection system, a pathologist can fast and accurately diagnose with certainty.

Despite these advances, there remain challenges to be addressed before AI-based histopathological image analysis becomes part of routine clinical practice. Deep learning algorithms rely on massive, high-quality, well-annotated datasets in order to be effective, except that such datasets are rare in the domain of medicine. In addition to these problems, challenges such as overfitting of the model, high cost of running the computation, and lack of interpretability, must also be addressed before models may be deployed within entire medical systems.

Histopathological images present their own special problems, the result of the numerous morphological mutations expressed in tumor tissues. For example, the various types of lung cancer, such as adenocarcinoma, squamous cell carcinoma, and small cell carcinoma, often have varying histological patterns which cannot readily be distinguished from one another. AI models must be capable of recognizing such differences and adapt to them without sacrificing accuracy. Yes you could use data augmentation or transfer learning which can help to circumvent the problem of variability, but once again only if the models have properly been trained and tested before applying those techniques.

The aim of this work is to evaluate and compare the performance of several state-of-the-art deep learning models, e.g., DenseNet121, VGG-19, Vision Transformers (ViT), Inception-V3, and ResNet-50, for lung cancer histopathology image classification. Our aim is to identify the optimal machine learning framework with the most accuracy and effectiveness by investigating these models specifically for the purpose of automated lung cancer detection in real-world guise that will result in improved diagnostic tools and patient outcomes.

2 Related works

Detection of lung cancer and lung nodules using deep convolution neural networks (CNNs) pulmonary disorder is described by P.K. Shimna, A. Shirly Edward, T.V. Roshini [1]. The study results showed that CNN-based models, capable of feature extraction and classification, could assist the diagnosis phase of histopathology image analysis. The authors ended their paper by stating that CNNs can be applied to enhance the automation of the detection and, consequently, reduce the dependence upon manual inspection, enabling advancing along the clinical path and decision making.

A lightweight end-to-end CNN model was proposed in [2] to automatically recognize different lung cancers by A. S. Sakr. The model is able to perform histopathological image analysis efficiently, and dynamically trade accuracy for computational complexity, thus can be used for real time diagnosis. Moreover low latency is introduced into the framework for the processing part of the pipeline and the latter runs within the reach for clinical constraints.

D. Z. Karim, T. A. Bushra[3] concentrated on lung cancer detection and they showed through the CNN that deep learning-based models have better performance than the traditional image processing models. Their method is an effective model capable of detecting cancerous areas in complex tissue images with a very high level of accuracy. Karim and Bushra emphasize data augmentation and preprocessing for enhanced classifier generalization.

U. Maheshwari, B. V. Kiranmayee, C. Suresh et al. [4] also employed pretrained machine learning techniques for the lung and colon cancers diagnosis. The results showed that transfer learning could discover meaningful classification relevance with small training data. Pre-trained models e.g. ResNet and VGG compared with models trained from scratch showed a significant improvement in feature extraction from medical images.

R. M. et al. [5] introduced a multi-level Convolutional Neural Network (CNN) to effectively classify lung cancer on histopathological images. They enhanced the feature learning by employing a multi-scale CNN model that could utilize other layers of the CNN simultaneously which make them more robust against image variations in the classification. They demonstrated how a hierarchy of architectures results in a the segmentation to capture low-level textures and progresses to high level semantics to make the classification more robust.

M. Anusha, D. S. Reddy [6] applied transfer learning by pre-trained models on ImageNet for the detection of lung and colon cancer. They discovered an efficient boosting in terms of classification accuracy and generalization among datasets and cold-start workability of different pre-trained networks when freezing some of the layers, particularly for scarce medical datasets.

R. I. Sumon et al. [7] compared several deep learning and machine learning models for detecting lung cancer based on her. The study said it's important to consider evaluation metrics that make sense in medical context (such as F1-score and ROC-AUC).

B. J. Ayekai et al. [8] proposed a histopathological image-based lung cancer prediction model based on the federated learning. Decentralized learning on the data also means that the data is private and everyone has an incentive to collaborate so that institutions can jointly train a model and use the data and keep their data private. The authors have argued that their approach could be valuable in a medical setting where sharing data is prevented by regulation concerning privacy.

G. Amirthayogam et al. [9] applied transfer learning for the lung and colon cancer diagnosis from histopathology images. They achieved good recall and precision values under their model, though it was a bit too expensive to be used on realistic--albeit extremely constrained--scenarios. They stressed the plasticity of deep learning models on large, heterogeneous datasets and one domain specific medical images fine tuning.

S. Mishra, U. Agarwal 10 proposed deep-convolutional neural nets to predict lung cancer from histopathological images, and optimized the convolutional layers in a layer-wise mannermake the model interpretable and performant. The authors employed attention mechanism for the model to concentrate attention towards important parts of images.

B. K. Hatuwal and H. C. Thapa [11] designed a CNN model for lung cancer detection with benchmarks, in which the architecture reported training and validation that this could be suitable for early-stage cancer detection. The framework as well includes post-processing operations such as morphological operations to assist in improving the segmentation of abnormal region.

S. Asif, V. Y. Wang, and D. Xu [12] recently developed a CT and adenocarcinoma histopathology image analysis model, using multi-level feature fusion with an attention mechanism. Their method would enhance diagnostic accuracy using a hybrid solution, which includes not only spatial information, but also context. This paper also reiterated that multimodal learning can improve the overall diagnostic efficacy markedly.

V. K. D. and M. G. [13] also developed a modified DEEP architecture model in cancer classification on lung and colon. The focus of the study is on methods for fine tuning and regularizing to get to a better classification result. Some of the optimization techniques include dropout layers, learning rate schedules, normalization methods of data.

M. Li et al. [14] proposed a histopathological image analysis for the auxiliary classification and diagnosis of lung cancer subtypes. For a more accurate subtype classification aiming at personalized treatment, they employed a visual feature plus metadata strategy. The extent the ensemble techniques contributed to enhancing the performance of the response classification was also quantified.

3 Data Description

The "Lung and Colon Cancer Histopathological Images" Kaggle repository, which is openly accessible, is the source of the dataset used in this work. The development and assessment of machine learning and deep learning models in the field of medical image classification—specifically, cancer diagnosis utilizing histopathology scans—is the focus of this dataset.

3.1 Dataset Composition

The original dataset comprises high-resolution histopathological images of both lung and colon tissue samples. How ever, for the purpose of this study, only the lung tissue subset was selected, and all colon-related samples were excluded. The focus on lung tissue was aimed at streamlining the model's learning process toward lung cancer detection and classification, reducing complexity while increasing specificity in training.

The lung subset is made up of 15,000 histopathological images in total, which have been carefully divided into three equal groups, each of which represents a different lung tissue condition:

3.1.1 Lung Benign Tissue (lung n): 5,000 images showcasing normal, non-cancerous lung tissue. These samples represent healthy lung cells and serve as the control group in the classification task. Fig 1 shows below.

3.1.2 Lung Adenocarcinoma (lung aca): five thousand pictures of cancerous lung tissue with glandular features. Known for its aggressive nature, adenocarcinoma is a prevalent subtype of non-small cell lung cancer (NSCLC) that starts in the cells lining the alveoli. Fig 2 shows below.

3.1.3 Lung Squamous Cell Carcinoma (lung scc): 5,000 images containing histological features of squamous cell carcinoma. This is another NSCLC subtype, originating from the squamous epithelial cells of the lung and often associated with smoking. Fig 3 shows below.

3.2 Image Characteristics

Every image in the collection is a high-resolution, high quality histopathology scan that has been pre-processed and stained with the Hematoxylin and Eosin (H&E) staining method. In order to improve visual analysis and automated feature extraction by deep learning models, this technique makes cellular structures more contrasted, making nuclei appear blue and other tissue components pink.

The images were annotated and labeled by certified pathologists and medical professionals to satisfy high data reliability and clinical relevance to the data. The high level of the annotation makes the dataset extremely useful for supervised learning tasks in the area of cancer diagnostics, where accuracy is paramount.

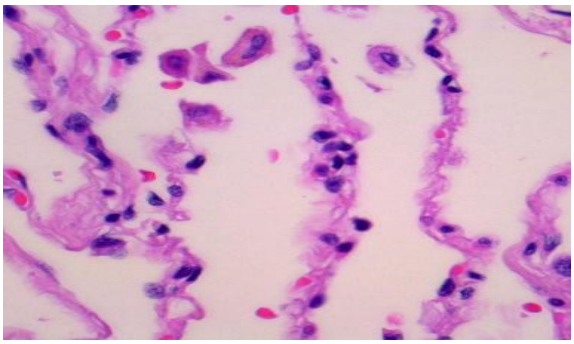

Fig. 1. Lung benign tissue.

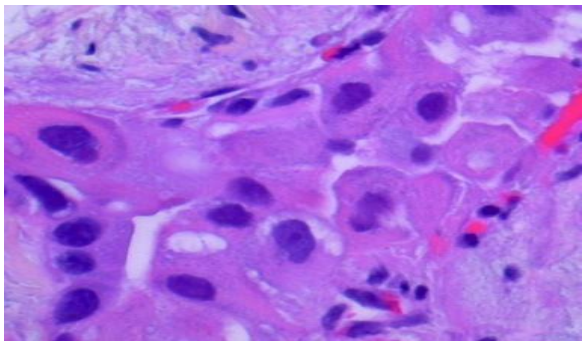

Fig. 2. Lung adenocarcinoma.

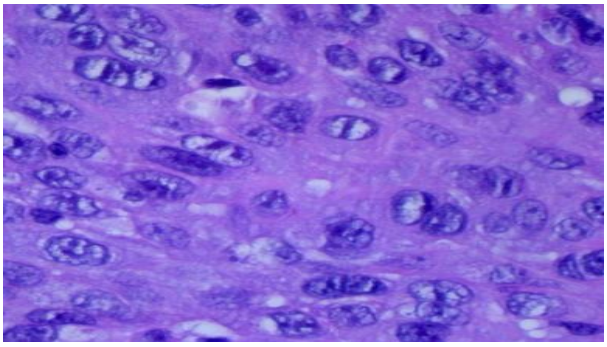

Fig. 3. Squamous Cell Carcinoma.

Represented above are histopathological images that are representative for each class. The benign tissues have uniformly structured cells showing low density. The adenocarcinomas have shown glandular dysplasia and enlarged nuclei while squamous cell carcinomas have disorganized clusters of hyperchromatic cells.

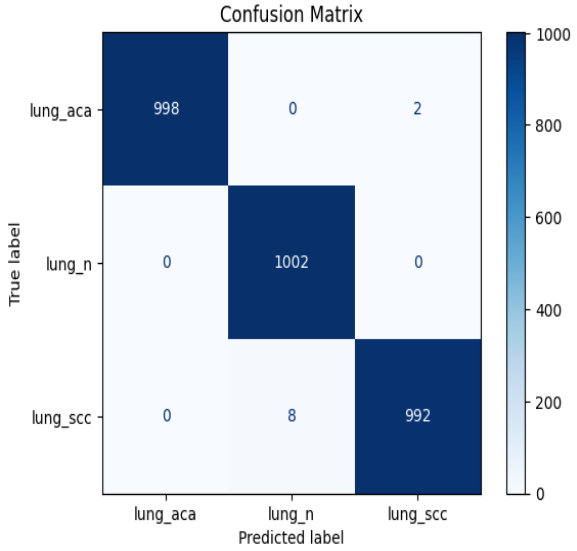

Fig. 4. Confusion matrix showing classification results for lung histopathological images.

Fig. 4 displays the confusion matrix that was created in order to assess how well the suggested model performed in identifying histological lung tissue pictures. In all three categories—Adenocarcinoma (lung aca), Squamous Cell Carcinoma (lung scc), and Normal (lung n) tissues—the matrix exhibits outstanding classification accuracy. Of the 1000 lung scc photos, the model accurately predicted 992 of them, all 1002 normal tissue samples, and 998 of 1000 lung aca images. Misclassifications were found to be minimal: eight lung scc samples were misclassified as lung n, and two lung aca samples were mislabeled as lung scc. These out comes demonstrate how well the model works and support the dataset's quality and balance.

4 Methodology

4.1 Preprocessing

Preprocessing data is a crucial stage in the medical im age analysis pipeline. To optimize downstream deep learning models' performance, preprocessing makes sure the input is formatted consistently, lowers variability, and improves pertinent features. We used a thorough preprocessing pipeline designed especially for the categorization of histopathology images in the diagnosis of lung cancer in this investigation. Fig 5 shows the preprocessing and augmentation flowchart.

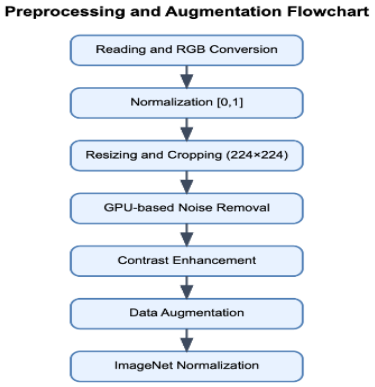

Fig. 5. Preprocessing and Augmentation Flowchart.

The following is an outline of the preprocessing steps:

- **RGB Conversion and Reading:** To ensure compatibility with pretrained CNN and transformer models, every histopathology image—which is usually in color format due to Hematoxylin and Eosin (HE) staining—is validated and standardized into RGB format.
- **Normalization:** To stabilize and speed up model training, pixel values are standardized to fall within [0, 1].
- **Resizing and Cropping:** To ensure consistent input size for model compatibility, images are scaled and center cropped to 224 × 224.
- **GPU-based Noise Removal:** In order to eliminate imaging noise and improve clarity, sophisticated denoising techniques with GPU acceleration are used.
- **Contrast Enhancement:** Histogram equalization and CLAHE are two methods used to enhance tissue contrast and cellular structure visibility.
- **Data Augmentation:** Training images are subjected to random rotations, color jittering, and flips in both the horizontal and vertical directions to increase the robustness of the model.
- **ImageNet Normalization:** For compatibility with pre trained model weights, a final normalization step is carried out using ImageNet statistics (μ = [0.485,0.456,0.406], σ = [0.229,0.224,0.225]).

After preprocessing, the complete dataset is split into subgroups for training (80%), validation (10%), and testing (10%). To guarantee data uniformity and integrity, the same preprocessing technique is performed consistently to each subset.

4.2 Model Selection Overview

We used top-performing deep learning models for this investigation, such as DenseNet121, VGG-19, Vision Transformers (ViT), Inception-V3, and ResNet-50, which are well known for their ability to classify histopathology images. These designs are well-established, reliable, and often suggested in literature and by frameworks such as MONAI, particularly DenseNet121, which is known for its exceptional accuracy, computational efficiency, and feature reuse in medical image analysis. Because of its exceptional capacity to identify lung cancer from histopathological pictures, DenseNet121 was selected as our main model.

4.2.1 ResNet-50

ResNet-50 is a model of a deep convolutional neural network that uses residual learning and has 50 layers. Residual learning uses skip connections, which give gradients a different way to backpropagate directly, to solve the vanishing gradient problem.

The residual block is defined by:

$$H(x) = F(x, W) + x \quad \ldots\ldots\ldots\ldots\ldots (1)$$

Where F (x, W) represents the residual mapping (usually a stack of two or three convolutions), and x is the input which is added back to the output of F. These identity mappings enable efficient training of very deep networks

Key Components:

- Bottleneck blocks with 1×1, 3×3, and 1×1 convolutions.
- Global average pooling followed by a dense classifier.

4.2.2 Inception-V3

Inception-V3 uses a “split-transform-merge” technique to collect spatial information at various scales by applying different kernel sizes to the same input feature map:

$$y = f_1(x) \oplus f_3(x) \oplus f_5(x) \quad \ldots\ldots\ldots\ldots\ldots (2)$$

In this case, $f_k(x)$ stands for a convolution with kernel size k × k, while $\oplus$ indicates concatenation channel. The model is able to acquire rich hierarchical features as a result.

Highlights:

- Factorized convolutions (e.g., 5 × 5 split into two 3 × 3)
- Auxiliary classifiers to support gradient flow
- Efficient computational cost with wide architectures

4.2.3 Vision Transformer (ViT)

The Vision Transformer makes use of picture patches in place of the transformer used in the field of natural language processing. Every picture is divided into patches of a set size, which are subsequently inserted as tokens and pass through layers of multi-head self-attention.

$$\text{Attention (Q, K, V)} = \text{softmax } \frac{QKT}{\sqrt{dk}} V \quad \ldots\ldots\ldots\ldots \quad (3)$$

where the values are denoted by V, the keys by K, and the queries by Q. This enables the full image's global contextual associations to be learned by the model.

Key Properties:

- No inductive biases (unlike CNNs)
- Position embeddings used to retain spatial information
- Long-range feature interaction.

4.2.4 VGG-19

VGG-19 is a deep convolutional network with 19 layers that emphasizes depth and simplicity. It uses a consistent architecture of stacked 3 × 3 convolutions and 2 × 2 max pooling:

$$F(x) = W_n (...ReLU(W_2(ReLU(W_1x+b_1)) +b_2) ...) \quad \ldots\ldots\ldots\ldots \quad (4)$$

Where each layer is followed by ReLU activation. Despite its large number of parameters, it is effective for transfer learning tasks.

Highlights:

- Uniform 3×3 kernel usage
- Simplicity and depth as a performance booster
- Commonly used as a baseline architecture.

4.2.5 Overview of DenseNet121

DenseNet121 is a deep learning model that prioritizes feature reuse and effective gradient flow. It stands for Densely Connected Convolutional Network with 121 layers. Layers in a standard convolutional neural network (CNN) combine data from one layer to the next without any feedback or links to earlier layers. DenseNet, on the other hand, feed-forwardly connects each layer to every other layer. The vanishing gradient issue is resolved and feature reuse is encouraged by giving each layer direct access to the gradients computed from the loss function and the original input signal.

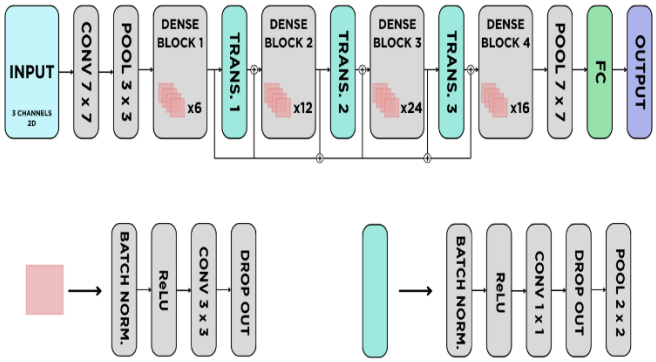

Fig. 6. DenseNet121 Architecture.

Fig 6 shows the dense net 121 architecture. A convolution and pooling layer are added at the beginning of DenseNet121, followed by four dense blocks that are divided by three transition layers and a classification head at the conclusion.

Input Layer: An initial convolutional layer is applied to the input image, which has dimensions of 224 × 224 × 3.

The network begins with a 7 × 7 convolutional layers comprising 64 filters and a stride of 2, capturing broad spatial features right from the input.

A Batch Normalization layer follows, coupled with a ReLU activation function to ensure faster convergence and non-linearity.

To reduce spatial dimensions and retain dominant features, a 3 × 3 Max Pooling layer with a stride of 2 is applied. Dense Blocks: DenseNet121 is architecturally structured into four densely connected blocks, where each block is made up of multiple composite layers that progressively refine feature representations:

- Dense Block 1: Consists of 6 composite layers.
- Dense Block 2: Expands with 12 composite layers.
- Dense Block 3: Deepens further with 24 composite layers.
- Dense Block 4: Finalizes with 16 composite layers.

Each composite layer is designed to maximize information f low and computational efficiency. It comprises the following sequence:

- Batch Normalization: Stabilizes learning by normalizing feature maps.
- ReLU Activation: Introduces non-linearity to improve representational capacity.
- 1×1Convolution (Bottleneck): Reduces dimensionality to improve efficiency.
- 3×3 Convolution: Extracts localized spatial features.

The output of each layer is concatenated with the outputs of all previous layers:

$x_l = H_l([x_0, x_1, ..., x_{l-1}])$ ……(5)

This structure enables rich feature reuse and mitigates the vanishing gradient issue. Transition Layers: Between dense blocks, transition layers perform down sampling and channel reduction:

- 1×1 Convolution
- 2×2 Average Pooling with stride 2

These layers control model complexity and reduce overfitting.

Classification Head: After the final dense block:

- A Global Average Pooling (GAP) layer compresses the spatial dimensions.
- A Fully Connected (Dense) layer maps to the output classes.
- A Softmax Activation function outputs class probability.

4.2.6 Advantages of Using DenseNet121 for Medical Imaging

For the following reasons, DenseNet121 has shown exceptional efficacy in medical image analysis, including the identification of lung cancer:

- **Efficient Feature Reuse:** Each layer accesses features from all preceding layers, leading to richer representations.
- **Improved Gradient Flow:** Helps with better training, especially with limited data.
- **Parameter Efficiency:** Requires fewer parameters compared to other deep models like ResNet.
- **Effective on Small Datasets:** Reduces overfitting by sharing weights and reusing features.
- **Strong Transfer Learning Base:** Can be easily fine-tuned from ImageNet pretrained weights for medical datasets.

5 Results and Evaluation

This section offers a comparison of various deep learning models for the categorization of lung cancer. Using training, validation, and test datasets, we compare the models in our study: DenseNet121, VGG-19, Vision Transformer (still ViT) Inception-V3, and ResNet-50.

5.1 Model Comparison

Table 1. Accuracy Comparison of Models.

Model	Train Acc. (%)	Val Acc. (%)	Test Acc. (%)
DenseNet121	**99.74**	**99.67**	**99.67**
VGG-19	98.40	97.80	97.42
ViT	96.15	95.78	94.38
Inception-V3	93.10	92.91	92.91
ResNet-50	85.77	84.64	84.64

Table 1 lists each model's accuracy metrics. DenseNet121 achieved training accuracy of 99.74%, validation accuracy of 99.67%, and test accuracy of 99.67%, outperforming all other models. Outstanding performance was also shown by VGG 19, which was followed by ViT, Inception-V3, and ResNet-50.

5.2 ROC Curve Analysis

The ROC (Receiver Operating Characteristic) curve for the DenseNet121 model illustrates almost perfect separability between the three classes of lung cancer. The AUC (Area Under Curve) values are all very close to 1.00, which confirms a high ability of the model to discriminate between classes in an unbiased way, consistently indicating a highly reliable classifier.

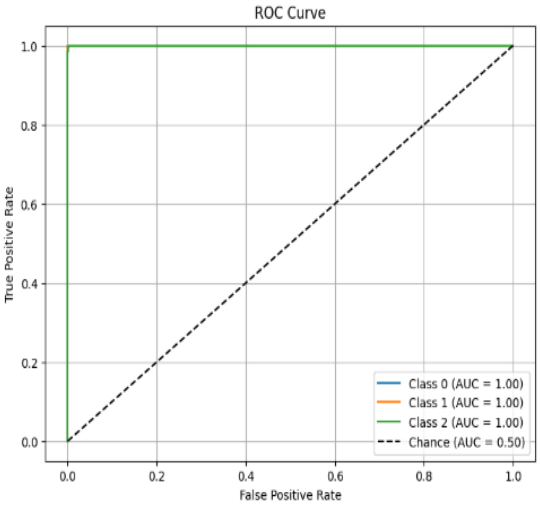

Fig. 7. ROC Curve for DenseNet121 across all classes.

Fig 7 illustrates the Receiver Operating Characteristic (ROC) curves for the three classes in our lung cancer classification task using DenseNet121, where each class—Class 0, Class 1, and Class 2—achieved a perfect Area Under the Curve (AUC) score of 1.00. This exceptional performance demonstrates the model's ability to distinguish between classes with high precision, minimizing both false positives and false negatives across the board. The ROC curve lies significantly above the diagonal line that represents random classification (AUC = 0.50), highlighting the superiority of our model. This near-perfect separation between the classes indicates not only a well-generalized model but also validates DenseNet121's reliability and potential in accurately supporting histopathological lung cancer diagnosis.

5.3 Training and Validation Loss/Accuracy

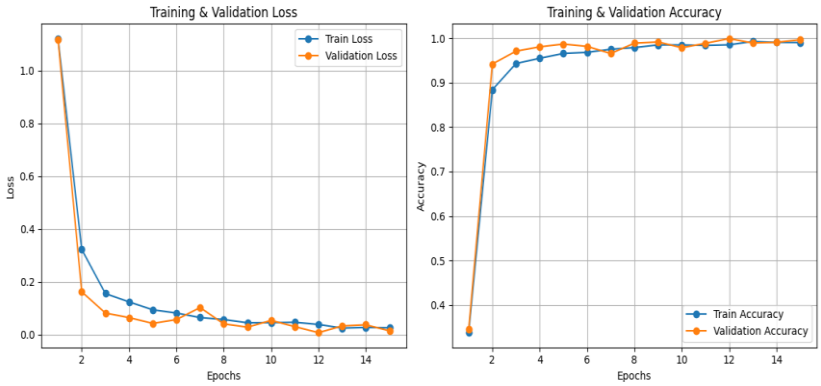

Fig. 8. Training and Validation Loss (left) and Accuracy (right).

Fig 8 shows the training and validation loss graphs (left) and accuracy graphs (right) show smooth progression with no signs of major overfitting. The model gains improvements through training, and generally performs similarly on validation data, which illustrates the generalizability and robustness of DenseNet121 in performing lung cancer image classification.

5.4 Classification Report

The classification report for the DenseNet121 model is shown in Fig 9. It obtained almost flawless F1-scores, recall, and precision in all three classes: lung aca, lung n, and lung scc. The model's great accuracy in identifying each form of lung cancer is demonstrated by these high scores.

```
Classification Report:
              precision    recall  f1-score   support

    lung_aca       1.00      1.00      1.00      1000
      lung_n       0.99      1.00      1.00      1002
    lung_scc       1.00      0.99      0.99      1000

    accuracy                           1.00      3002
   macro avg       1.00      1.00      1.00      3002
weighted avg       1.00      1.00      1.00      3002
```

Fig. 9. Classification Report for DenseNet121.

The weighted average, macro average, and overall accuracy all hit 1.00. DenseNet121's balanced performance on both common and less frequent classes is highlighted by its consistency across measures. Its dependability for clinical picture classification tasks is confirmed by the findings.

6 Conclusion

In this study, we explored the application of deep learning techniques for the classification of lung cancer using histopathological images, leveraging well-established architectures including DenseNet121, VGG-19, Vision Trans former (ViT), Inception-V3, and ResNet-50. Among them, DenseNet121 consistently outperformed the others across all evaluation metrics, achieving near-perfect AUC scores and over 99% accuracy in training, validation, and test phases. Its ability to effectively learn complex features, maintain generalization, and avoid overfitting underscores its suitability for medical image analysis, particularly in detecting lung cancer subtypes from histopathological scans. In contrast, models like ResNet-50 and Inception-V3 showed relatively lower performance, highlighting the critical role of architectural depth and connectivity in capturing the morphological nuances of cancerous tissues. The comprehensive evaluation confirmed DenseNet121's robustness across all classes with balanced precision, recall, and F1-scores. While the results are promising, the study acknowledges limitations such as potential dataset bias and the exclusive use of image-based inputs; future work could benefit from integrating multimodal data sources, including clinical reports and genomic information, to further enhance diagnostic accuracy and reliability. Overall, this research reinforces the potential of deep learning, particularly DenseNet121, as a powerful tool for augmenting histopathological lung cancer diagnosis and supporting clinical decision-making.

References

[1] P. K. Shimna, A. Shirly Edward, and T. V. Roshini," A Review on Diagnosis of Lung Cancer and Lung Nodules in Histopathological Images using Deep Convolutional Neural Network," 2023 International Conference on Artificial Intelligence and Applications (ICAIA) Alliance Technology Conference (ATCON-1), 2023, pp. 1-4. doi:10.1109/ICAIA57370.2023.10169738.

[2] A. S. Sakr," Automatic Detection of Various Types of Lung Cancer Based on Histopathological Images Using a Lightweight End-to-End CNN Approach," 2022 20th International Conference on Language Engineering (ESOLEC), 2022, pp. 141-146. doi:10.1109/ESOLEC54569.2022.10009108.

[3] D. Z. Karim and T. A. Bushra," Detecting Lung Cancer from Histopathological Images using Convolution Neural Network," TENCON 2021, pp. 626-631. doi:10.1109/TENCON54134.2021.9707242.

[4] U. Maheshwari, B. V. Kiranmayee, and C. Suresh," Diagnose Colon and Lung Cancer Histopathological Images Using Pre-Trained Machine Learning Model," 2022 IC3I, pp. 1078-1082. doi:10.1109/IC3I56241.2022.10073184.

[5] R. M, M. S, T. S, K. K, L. Krishnasamy, and S. N," Efficient Lung Cancer Classification on Multi level Convolution Neural Network using Histopathological Images," 2023 ICCCNT, pp. 1-7. doi:10.1109/ICCCNT56998.2023.10307852.

[6] M. Anusha and D. S. Reddy," Enhancing Lung and Colon Cancer Diagnosis: An ImageNet-Trained Transfer Learning Approach for Histopathological Image Analysis," 2024 ICBSII, pp. 1-4. doi:10.1109/ICBSII61384.2024.10564039.

[7] R. I. Sumon, M. A. I. Mazumdar, S. M. I. Uddin, and H.-C. Kim," Exploring Deep Learning and Machine Learning Techniques for Histopathological Image Classification in Lung Cancer Diagnosis," 2024 ICECET, pp. 1-6. doi:10.1109/ICECET61485.2024.10698211.

[8] B. J. Ayekai et al.," Federated Lung Cancer Prediction Using Histopathological Medical Images," 2022 ICCWAMTIP, pp. 1-6. doi:10.1109/ICCWAMTIP56608.2022.10016519.

[9] G. Amirthayogam, S. S, G. Maheswari, M. James, and K. Remya," Lung and Colon Cancer Detection using Transfer Learning," 2024 ICONSTEM, pp. 1-6. doi:10.1109/ICONSTEM60960.2024.10568787.

[10] S. Mishra and U. Agarwal," Lung Cancer Detection (LCD) from Histopathological Images Using Fine-Tuned Deep Neural Network," Proceedings of ICICCIS 2022, 2023.
[11] B. K. Hatuwal and H. C. Thapa," Lung Cancer Detection Using Convolutional Neural Network on Histopathological Images," International Journal of Computer Trends and Technology, vol. 68, no. 10, pp. 21-24, 2020. doi:10.14445/22312803/IJCTT-V68I10P104.
[12] S. Asif, V. Y. Wang, and D. Xu," LungX-Net: Lung Cancer Diagnosis from CT and Histopathological Images via Attention Based Multi-Level Feature Fusion Network," 2024 IEEE BIBM, pp. 6334-6341. doi:10.1109/BIBM62325.2024.10822200.
[13] V. K. D. and M. G.," Optimized Deep Learning Approaches for Lung and Colon Cancer Classification using Histopathological Images," 2024 ICACRS, pp. 1665-1669. doi:10.1109/ICACRS62842.2024.10841547.
[14] M. Li et al.," Research on the Auxiliary Classification and Diagnosis of Lung Cancer Subtypes Based on Histopathological Images," IEEE Access, vol. 9, pp. 53687-53707, 2021. doi:10.1109/ACCESS.2021.3071057.